ELSEVIER

Journal of Fluids and Structures 26 (2010) 764–779

JOURNAL OF FLUIDS AND STRUCTURES

www.elsevier.com/locate/jfs

Experimental observation of single mode panel flutter in supersonic gas flow

Vasily V. Vedeneev[a,*], Sergey V. Guvernyuk[a], Alexander F. Zubkov[a], Mikhail E. Kolotnikov[b]

[a]*Lomonosov Moscow State University, Faculty of Mechanics and Mathematics, 1 Leninskie Gory, Moscow, Russia*
[b]*Moscow Machine Building Product Plant "Salut", 16 Budionny Av., Moscow, Russia*

Received 10 September 2009; accepted 5 April 2010
Available online 22 June 2010

Abstract

Single mode flutter is a type of panel flutter, which cannot be analyzed theoretically using conventional piston theory, and for this reason it is studied very little. No previous experiments, where this type of panel flutter was clearly detected, were conducted. In this paper a plate, designed such that it cannot experience "classical" coupled-mode type flutter, but can experience single mode flutter, is tested. Analysis of the tested data clearly indicates the occurrence of single mode panel flutter.

Keywords: Panel flutter; Plate flutter; Single mode flutter; Vibrations; Aeroelasticity

1. Introduction

Panel flutter is an aeroelastic phenomenon that is known to cause fatigue damage of flight vehicles. Consider a skin panel of a flight vehicle in a supersonic gas flow, for example, a wing skin panel (Fig. 1). If the flow speed is relatively low, then the static state of the panel is stable. Once the critical speed (or the critical Mach number, M_{cr}) is exceeded, the static state of the panel becomes unstable, and the panel vibrates. This vibration occurs due to energy transfer from the gas flow to the panel. The amplitude of this vibration can be large and result in fatigue damage of the panel and the structures attached to the panel.

This problem of panel flutter was first observed during the 1940s and has since had a very rich history. Theoretical solution of the problem consists of an eigenvalue solution of coupled panel-flow equation. Let us assume that the plate deflection is harmonic: $w(x,t) = W(x)e^{-i\omega t}$ (for simplicity we demonstrate the theory on 2-D problem), the dimensionless equation of the plate motion takes the form

$$D\frac{\partial^4 W}{\partial x^4} - \omega^2 W + p\{W,\omega\} = 0, \tag{1}$$

*Corresponding author. Tel.: +7 916 338 23 82.
E-mail addresses: vasily@vedeneev.ru (V.V. Vedeneev), guv@mail.ru (S.V. Guvernyuk), kolotnikov@salut.ru (M.E. Kolotnikov).
URL: http://www.vedeneev.ru (V.V. Vedeneev).

0889-9746/$ - see front matter © 2010 Elsevier Ltd. All rights reserved.
doi:10.1016/j.jfluidstructs.2010.04.004

where D is the dimensionless plate stiffness, and $p\{W,\omega\}$ is the pressure acting on the oscillating plate. The potential gas flow theory gives the following expression (Bolotin, 1963):

$$p\{W,\omega\} = \frac{\mu M}{\sqrt{M^2-1}}\left(-\mathrm{i}\omega W(x) + M\frac{\partial W(x)}{\partial x}\right) + \frac{\mu\omega}{(M^2-1)^{2/3}}\int_0^x \left(-\mathrm{i}\omega W(\xi) + M\frac{\partial W(\xi)}{\partial \xi}\right)\exp\left(\frac{\mathrm{i}M\omega(x-\xi)}{M^2-1}\right)\left(\mathrm{i}J_0\left(\frac{-\omega(x-\xi)}{M^2-1}\right) + MJ_1\left(\frac{-\omega(x-\xi)}{M^2-1}\right)\right)\mathrm{d}\xi, \quad (2)$$

where M is the Mach number, and μ the air density to plate material density ratio. Substitution of this expression into Eq. (1) yields the complex integro-differential equation. Solving this equation is difficult; however, in the 1950s a relatively simple theory, known as the piston theory, was developed to approximate the gas pressure. This theory, shown in Eq. (3), neglects the integral terms from Eq. (2), therefore it is valid only at high Mach numbers and low frequencies:

$$p\{W,\omega\} = \frac{\mu M}{\sqrt{M^2-1}}\left(-\mathrm{i}\omega W(x) + M\frac{\partial W(x)}{\partial x}\right). \quad (3)$$

This partial-differential Eqs. (1), (3) can be easily solved numerically and studied analytically. Piston theory has been the primary analysis method used by aeroelasticians. An enormous number of panel flutter publications have used the more simplistic piston theory but only a few authors have published work regarding the exact theory of potential flow (Nelson and Cunnigham, 1956; Dun Min-de, 1958; Dowell, 1967, 1971; Yang, 1975; Dong Ming-de, 1984). Up to the present day, the focus of most studies of panel flutter is in regard to complications related to structure design, whereas air pressure is calculated using piston theory (3).

Though piston theory is a simple approach used to predict flutter, it also has a serious problem. Two types of panel flutter are known (Dowell, 1974). First, the coupled-type flutter arising due to the interaction of two eigenmodes (Fig. 2(a)). This type has been fully studied through the piston theory, and excellent correlation with experiments at $M>1.7$ has been observed. The second flutter type is single mode flutter also referred as "single-degree-of-freedom" or "high-frequency" flutter (Fig. 2(b)). This flutter type can only be analyzed through exact aerodynamic theory of potential flow or more complex theories. Until recently, only in a few publications single mode flutter was mentioned (Nelson and Cunnigham, 1956; Dowell, 1967, 1974), where it was obtained through direct numerical simulations; however, the energy transfer mechanism was not studied.

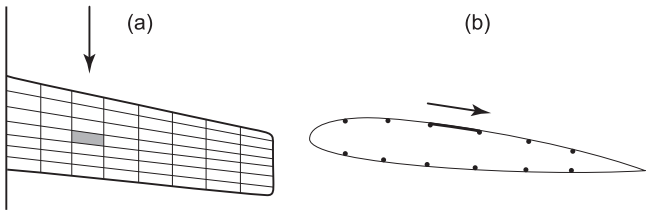

Fig. 1. Skin panel is a typical structure subjected to panel flutter.

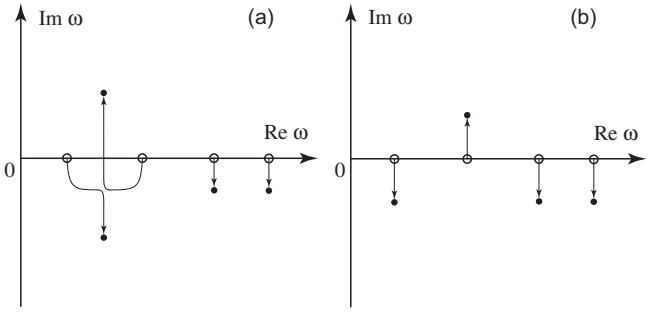

Fig. 2. Trajectories of eigenfrequency loci in the complex ω plane during changing of critical problem parameter (Mach number, for example). Bottom half-plane is stability region, top half-plane is flutter region. (a) Coupled-mode type flutter, (b) single mode flutter.

Table 1
Eigenmodes which are unstable in region $M<1.3$ and their flutter regions.

m	n	Frequency Ω (Hz)	M_1	M_2
1	1	65	1.19	1.56
2	1	167	1.17	1.48
2	2	190	1.28	1.61
3	1	321	1.20	1.48
3	2	344	1.26	1.54
4	1	526	1.25	1.49
4	2	549	1.29	1.53

This flutter type has not been thoroughly investigated, and some have even suggested that it may not occur in reality. However, over the past few years single mode flutter was studied in detail in Vedeneev (2005, 2006, 2007, 2009), and a simple physical explanation of the instability has been derived.

The usual explanation of single mode flutter is "negative aerodynamic damping". Expansion of (2) at low frequencies yields

$$p\{W,\omega\}=\frac{\mu M}{\sqrt{M^2-1}}\left(-\mathrm{i}\omega\frac{M^2-2}{M^2-1}W(x)+M\frac{\partial W(x)}{\partial x}\right)+o(\omega^2) \tag{4}$$

Evidently, the first fraction of the parentheses, which represents aerodynamic damping, is negative if $M<\sqrt{2}$, and in this case formula (4) always predicts single mode instability. This is a very simple and basic way to represent single mode flutter. Theory presented herein and in Vedeneev (2005, 2006, 2007, 2009) provides higher accuracy, which still yields a closed-form solution. This theory gives two significant improvements of single mode flutter criteria $M<\sqrt{2}$. First, even for the 2-D problem there is its unique region of instability for each mode, $M_1<M<M_2$ (for example, see Table 1). For higher modes the upper flutter boundary, M_2, is higher than $\sqrt{2}$, moreover $M_2\to\infty$ as the mode number tends to infinity. Thus, theoretically, single mode flutter can occur at any arbitrary M at appropriate high-frequency mode. But this, of course, cannot be realized at very high M, due to strong damping of high-frequency modes. For the 3-D problem (rectangular plate) M_2 differs from $\sqrt{2}$ even for low-frequency modes. Another improvement is that the theory presented here yields significantly different stability boundary in case when in-plane tension of the plate is present. Formula (4), of course, is not able to capture this effect and always gives single mode flutter criteria $M<\sqrt{2}$ in both 2-D and 3-D cases.

Several important studies on the boundary layer effect on panel flutter have been conducted (Dowell, 1971); see also bibliography in Dowell (1974). It has been shown that a thick boundary layer can significantly change the flutter boundary. This, however, has no relation to the tests presented here, as the boundary layer thickness was very small (see details below).

While there have been a few prior experimental studies of single mode panel flutter, conducted at NASA Ames Research Center (Muhlstein et al., 1968; Gaspers et al., 1970), the present study is more comprehensive in its scope and includes an in-depth discussion of the physical phenomena from both experimental and theoretical points of view.

This paper explains the analysis method and experiments conducted to confirm the existence of single mode flutter. Tests focusing on single mode flutter have been conducted at the Institute of Mechanics of Moscow State University. These experiments used a clamped plate, which has been designed such that coupled-type flutter cannot occur during wind tunnel testing. At the same time, single mode flutter should occur. Gauges used during the experiment allow for monitoring of the plate vibrations and the vibration source. The results clearly show that the plate vibrations confirm the existence of single mode flutter.

2. Theoretical considerations

Firstly we will consider theories used to predict panel flutter of rectangular plates.

2.1. Coupled-mode type panel flutter

Let us assume that Mach number M is high, and the piston theory (3) can be used. Then the panel flutter eigenvalue problem takes the form

$$D\Delta^2 W-\omega^2 W+\frac{\mu M}{\sqrt{M^2-1}}\left(-\mathrm{i}\omega W(x)+M\frac{\partial W(x)}{\partial x}\right)=0, \tag{5}$$

supplemented with appropriate boundary conditions at the plate edges.

In Movchan (1957) eigenvalue problem (5) was studied analytically for the plate having all edges simply supported:

$$W=\frac{\partial^2 W}{\partial x^2}=0,\quad x=\pm L_x/2,\quad W=\frac{\partial^2 W}{\partial y^2}=0,\quad y=\pm L_y/2.$$

The following flutter criterion was obtained:

$$M>M_{\mathrm{cr}}=\frac{D}{p\gamma L_x^3}\frac{8\pi^3}{3\sqrt{3}}\left(5+\frac{L_x^2}{L_y^2}\right)\sqrt{2+\frac{L_x^2}{L_y^2}}, \tag{6}$$

where L_x and L_y are the plate width and length (air flows along the x direction), D is the plate stiffness, p is a static pressure of the flow, γ is an adiabatic constant of the air (in this formula all parameters are dimensional). It is shown analytically that for the plate having some of the edges clamped and some pinned the critical Mach number is higher than given by (6).

Other boundary conditions were studied numerically in numerous papers (Hedgepeth, 1957; Dowell and Voss, 1965; Dugundji, 1966; Dowell, 1966).

Flutter which is observed in all the papers using piston theory is a coupled-mode type flutter. Indeed, let us consider motion of the plate eigenfrequencies in the complex ω plane. If the Mach number is not very high, and the plate is stable, all eigenfrequencies are located in the bottom ω half-plane. Let us now increase Mach number (or change any other parameter leading to flutter). The first and the second eigenfrequencies move toward each other, almost merge, and then go away from each other in vertical directions (Fig. 2(a)). Thus, interaction of two eigenmodes occurs. Physically this interaction of the plate eigenmodes happens through the effect of the air flow.

Studies devoted to the accuracy of piston theory (Bolotin, 1963) show that piston theory may be used for $M>1.7$. At lower Mach numbers error becomes significant, and more precise theory should be used.

Coupled-mode type panel flutter was observed in many experiments, and at high Mach numbers the theoretical flutter boundary gives an excellent prediction (Mikishev, 1959; Dowell and Voss, 1965). During the past years numerous papers devoted to nonlinear flutter studies have been published (Mei et al., 1999). In most of them piston theory is used for calculation of air pressure, and flutter appeared in these papers is a coupled-mode type flutter.

2.2. Single mode flutter

Single mode flutter is a flutter that occurs without interaction of two or more eigenmodes. It was first observed by Nelson and Cunnigham (1956), where air pressure was calculated using potential gas flow theory . Then it was observed at low Mach numbers by Dowell (1967, 1971). In these papers the eigenvalue problem was studied numerically. There are no studies of energy transfer mechanism from the flow to the plate.

In Vedeneev (2006) single mode flutter was studied analytically using the asymptotical method of global instability (Kulikovskii, 1966, 2006), and a physical explanation of flutter excitation was obtained. Let us consider a natural oscillation mode of a pinned plate in vacuum:

$$w(x,y,t)=\cos(k_x x)\cos(k_y y)\mathrm{e}^{-\mathrm{i}\omega t}. \tag{7}$$

Rewriting this formula, we obtain

$$\begin{aligned} w(x,y,t)&=\tfrac{1}{4}(\mathrm{e}^{\mathrm{i}k_x x}+\mathrm{e}^{-\mathrm{i}k_x x})(\mathrm{e}^{\mathrm{i}k_y y}+\mathrm{e}^{-\mathrm{i}k_y y})\mathrm{e}^{-\mathrm{i}\omega t}\\ &=\tfrac{1}{4}(\mathrm{e}^{\mathrm{i}(k_x x+k_y y-\omega t)}+\mathrm{e}^{\mathrm{i}(k_x x-k_y y-\omega t)}+\mathrm{e}^{\mathrm{i}(-k_x x-k_y y-\omega t)}+\mathrm{e}^{\mathrm{i}(-k_x x+k_y y-\omega t)}). \end{aligned} \tag{8}$$

Each term in (8) is a plane wave moving along the plate. Thus, natural oscillation of the plate can be represented as a superposition of four plane waves. Let us describe how this superposition occurs.

First, consider a single plane wave moving along an imaginary infinite plate with wave vector $\{k_x,k_y\}=\{k\cos\alpha,k\sin\alpha\}$. Here α is an angle between the gas flow and wave vectors, $k=\sqrt{k_x^2+k_y^2}$, $\mathrm{Re}(k)>0$. In the absence of air, k is real and positive; in the presence of air k is generally complex. Positive $\mathrm{Im}(k)$ corresponds to spatial damping of the wave, and a negative one corresponds to spatial amplification.

The dispersion relation connecting k and ω of an infinite plate–air system free from in-plane force has the form (Vedeneev, 2005, 2006)

$$(Dk^4-\omega^2)-\mu\frac{(\omega-Mk\cos\alpha)^2}{\sqrt{k^2-(\omega-Mk\cos\alpha)^2}}=0. \tag{9}$$

Here μ is a ratio of air density to the plate material density. Denoting $k_0(\omega)=k(\omega,\mu=0)$ (wave vector length in the absence of air) and considering μ as a small parameter, from (9) we obtain

$$k(\omega,\mu)=k_0+\Delta(k_0),$$

where $\Delta(k_0)$ is the first term of expansion $k(\mu)$ at small μ. The behaviour of $\Delta(k_0)$ is defined by the phase velocity of the wave $c_0=\omega/k_0$ (Vedeneev, 2005). If $c_0<M\cos\alpha-1$ then $\mathrm{Im}(\Delta(k_0))$ is negative; if $M\cos\alpha-1<c_0<M\cos\alpha+1$ it is equal to zero; if $c_0>M\cos\alpha+1$ then it is positive. At $c_0\approx M\cos\alpha\pm1$ order of $\Delta(k_0)$ is $\mu^{2/3}$, otherwise it has order of μ. Consequently, the most amplification of the wave occurs at $c_0\approx M\cos\alpha-1$, while the most damping occurs at $c_0\approx M\cos\alpha+1$.

Let us consider the meaning of these inequalities. Decompose the air velocity vector into a component lying in the wave plane and a normal-to-plane component. Flow in the direction normal to the wave plane occurs with Mach number $M\sin\alpha$ and does not affect the wave. Flow in the wave plane has a Mach number $M\cos\alpha$ and drives the action of air on the wave along the plate. If $c_0<M\cos\alpha-1$ then air flow is supersonic with respect to the wave, and the flow direction with respect to the wave coincides with direction of the wave motion. At $M\cos\alpha-1<c_0<M\cos\alpha+1$ air motion with respect to the wave is subsonic. At $c_0>M\cos\alpha+1$ the air flow is supersonic again, but the flow direction with respect to the wave is opposite to the wave motion. Now, if we consider the phase shift between the wave moving along the plate and air pressure acting on this wave, and calculate the work done by the pressure, we will obtain the following: at $c_0<M\cos\alpha-1$ this work is positive, i.e. $\mathrm{Im}(\Delta(k_0))<0$; at $M\cos\alpha-1<c_0<M\cos\alpha+1$ the work equals to zero, i.e. $\mathrm{Im}(\Delta(k_0))=0$; and at $c_0>M\cos\alpha+1$ the work is negative, i.e. $\mathrm{Im}(\Delta(k_0))>0$. At $c_0=M\cos\alpha\pm1$ resonance between a wave moving along the air with speed $M\cos\alpha\pm1$ (fronts of acoustic waves) and along the plate with speed c_0 occurs. This resonance is the reason of the most amplification and most damping of the wave at these values of c_0.

Let us now go back to the eigenmode (8) and study influence of the air on the eigenmode. For this purpose it is convenient to represent the motion of each wave as a motion of its separate segments (Fig. 3). Between the edges the trajectories of these segments are rectilinear with one of the four directions (Fig. 4), and from the edges mirror reflection occurs. Depending on the oscillation mode considered, the trajectories may be closed (Fig. 5(a) and (b)) or open (Fig. 5(c)). The closed trajectory is a closed broken line. It is easy to show that the open trajectory is everywhere dense in the rectangle defined by the plate contour.

We will call the period in which the wave segment trajectories return to their initial position (if the trajectory is closed) or close to it (if open) the wave segment reflection cycle. We will consider a certain trajectory and calculate the change in amplitude per reflection cycle. The amplitude changes, firstly during wave motion from one edge to another due to the presence of the imaginary part of the wavenumber (motion along trajectory segments), and secondly during reflection from the plate edges. Considering successively the changes in amplitude during motion between the edges and during reflection and assuming that the initial amplitude is equal to unity and that in this time n reflections occur, we find the amplitude after the reflection cycle:

$$\prod_{p=1}^{n} A_p \mathrm{e}^{-l_1\mathrm{Im}(\Delta(k_1))-l_2\mathrm{Im}(\Delta(k_2))-l_3\mathrm{Im}(\Delta(k_3))-l_4\mathrm{Im}(\Delta(k_4))}. \tag{10}$$

Here A_i are the coefficients of reflection from the edges and l_j are the total distances traversed by the trajectory in the j-direction. If the value of (10) is more than 1, then the plate eigenmode amplifies after the reflection cycle, otherwise it damps. Since in the absence of a gas the amplitude does not change after the reflection cycle (the plate itself is a conservative system), then $\prod_{p=1}^{n} A_p=1$. Also, $l_1=l_3$, $l_2=l_4$ (in the case of an open trajectory these equalities hold approximately true). Since the gas flow vector is parallel to the x axis, due to the symmetry $\Delta(k_1)=\Delta(k_2)$, $\Delta(k_3)=\Delta(k_4)$. Therefore, the oscillation amplification condition takes the final form

$$\mathrm{Im}(\Delta(k_1))<-\mathrm{Im}(\Delta(k_3)) \tag{11}$$

Since the trajectories differ from each other only with respect to the initial point and coincide in the direction of motion, the change in amplitude after a reflection cycle and condition (11) are independent of the trajectory and are determined only by the oscillation mode.

Flutter criterion (11) allows a determination of whether a chosen plate natural mode is amplified by the air flow or not. We emphasize that this analysis should be applied to each plate natural mode. Detailed study shows that regularly at the same parameters there are several plate oscillation modes subjected to flutter. This fact was noticed in Bendiksen and Davis (1995) and Bendiksen and Seber (2008), where flutter at $M>1$ occurred at higher modes. In Vedeneev (2006) this fact is explained using the simple analysis described above.

Another feature of single mode flutter is the fact that flutter criterion (11) does not depend on μ. Indeed, in case of coupled-type flutter a high value of μ (in dimensional terms, air density or air pressure) is required for two modes to interact. However, in case of single mode flutter no mode interaction occurs. If μ is very low, then the plate still flutters,

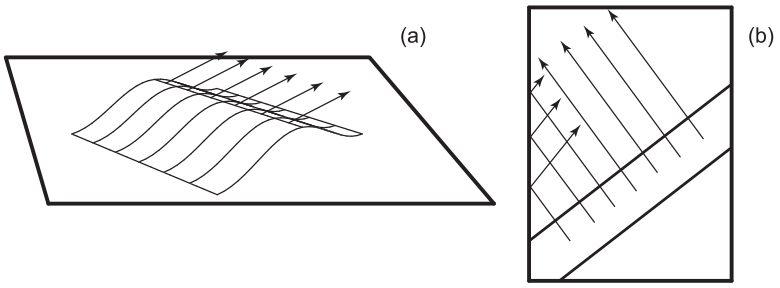

Fig. 3. (a) Representation of the wave motion as the motion of its individual segments and (b) the initial trajectories of these segments.

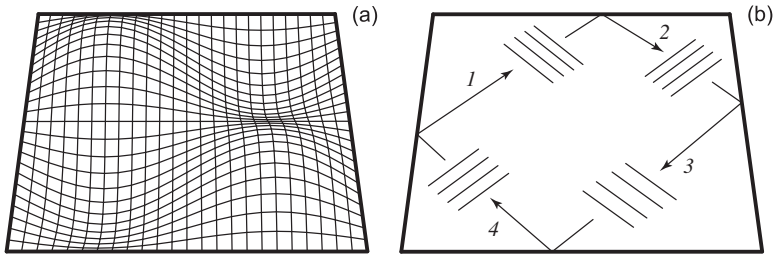

Fig. 4. Natural plate oscillation mode—(a) standing wave and (b) its representation as a superposition of four travelling waves.

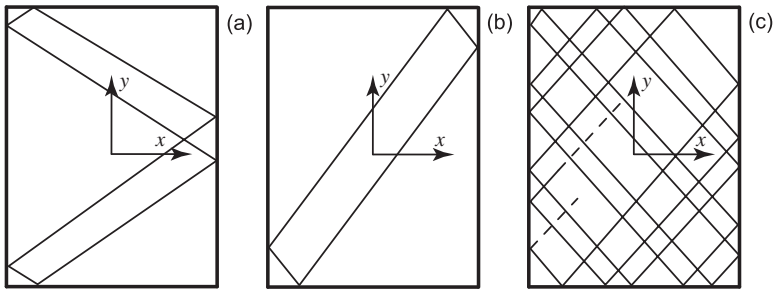

Fig. 5. Wave segment trajectories: (a) closed trajectory symmetrical about one of the coordinate axes, (b) closed trajectory asymmetrical about the coordinate axes, (c) open trajectory.

but the rate of mode amplification (10) is very low. This fact was obtained numerically in Dowell (1967), where the plate fluttered at very low air pressure.

To date, there are no records where single mode flutter was observed in experiment. That is why it is important to conduct such a test and study experimentally single mode panel flutter.

3. Description of the experiment

The experiment set-up is shown in Fig. 6. The tested specimen is a flat plate made from steel and welded to a rigid frame. The frame has been fixed to the wind tunnel wall. The plate size was $300 \times 540 \times 1$ mm in the x (flow), y (side) and z directions. A cavity under the plate allows for gas flow to bypass under the plate, which equalizes the pressure between the two sides of the plate. The wind tunnel dimension is 600×600 mm. Its design is such that during transonic regimes there is always some suction through perforated tunnel walls. Therefore, a boundary layer is absent on the permeable tunnel wall and appears only at the short segment of the model and can be neglected. Typical air parameters of the experiment are: total pressure is 112–142 kPa, total temperature is 279–286 K.

To monitor plate vibrations, 12 strain gauges were installed on the "cavity" side of the plate (Fig. 7). The gauge signals were amplified and operated in the range of 20–10 000 Hz. A vibro gauge AP2037 was installed outside the

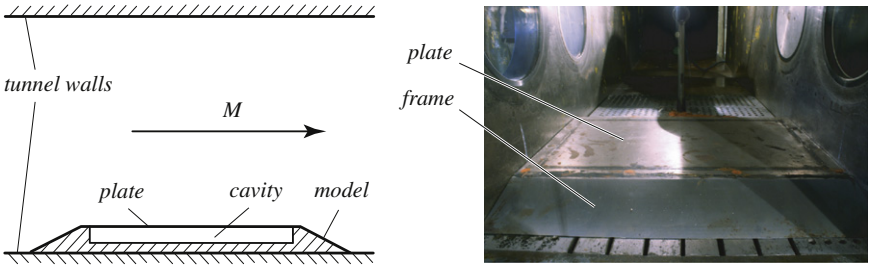

Fig. 6. Sketch of the test (left). Picture of the model installed into the tunnel (right).

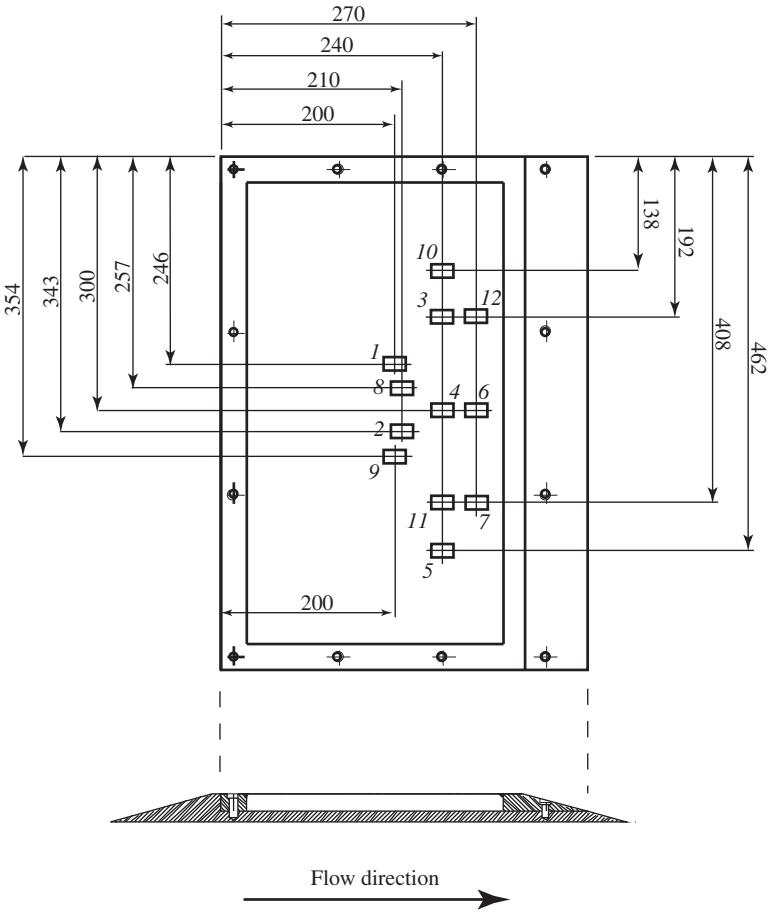

Fig. 7. Strain gauges installed on the plate.

tunnel wall to monitor wind tunnel vibrations. This gauge was used with transformer AS02. Flow pressure pulsations were monitored by means of a Honeywell pressure gauge 186PC15DT. Fig. 8 depicts the set-up configuration by which measurements have been taken during the experiment.

Generally, five sources of high-amplitude plate oscillations could occur during the test:

(i) resonance excited by vibrations of the wind tunnel;
(ii) resonance excited by pulsations of the flow pressure;
(iii) response to noise excitation;
(iv) coupled-type panel flutter;
(v) single mode panel flutter.

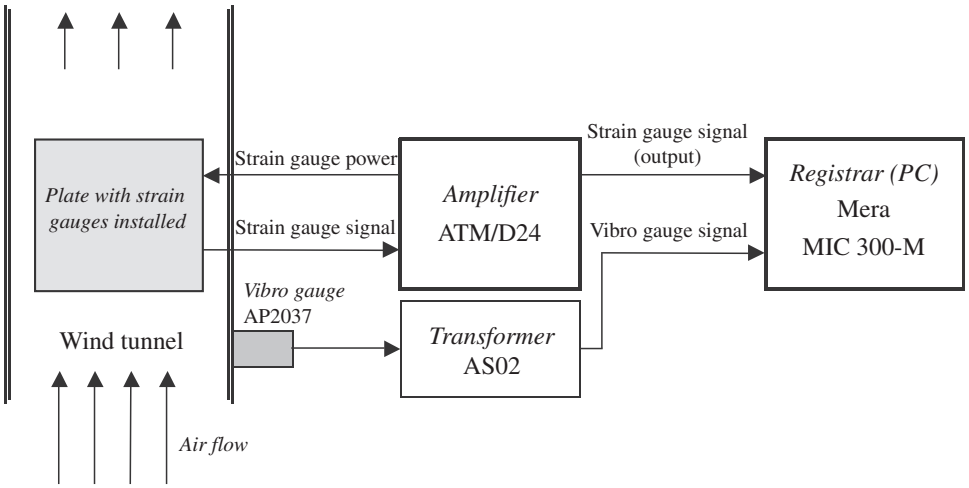

Fig. 8. Scheme of the test measurements (pressure gauge is not shown).

Identifying the actual plate vibrations type is possible through spectral analysis of the plate strain gauges, tunnel vibro gauge and the pressure gauge spectrum data. Special discriminants can be used to exclude or confirm the types of plate oscillations; they are described in following.

Resonance excited by vibrations of the wind tunnel can be easily recognised by comparing the spectra of the plate strain gauges and the tunnel vibro gauge. If high-amplitude peaks exist in these spectra with the same frequencies, then the wind tunnel has caused the plate vibrations. On the contrary, if the plate oscillates at a different frequency than that of the vibro gauge, then the first type of vibrations is likely to be excluded, barring possible nonlinear excitation from other strong wall vibration modes.

In the same way, resonance excited by pulsations of the flow pressure can be easily detected by comparing spectra of the plate strain gauges and the flow pressure gauge.

Noise excitation of the plate vibrations can be detected comparing vibration amplitudes at several regimes of the wind tunnel (for example, at several Mach numbers). If while changing Mach number, M, both the amplitudes of noise vibrations of the tunnel and noise pulsations of the flow pressure increase, while amplitude of the plate vibrations decreases or increases at a much faster rate than the noise amplitude (or *vice versa*), then these vibrations cannot be caused by noise excitation.

Coupled-mode type flutter can be detected using its main feature: it occurs due to interaction of two eigenmodes, which can be detected by the approaching and coalescence of the first and the second eigenfrequencies. Thus, if the amplitude increases sharply, while the two mentioned eigenfrequencies do not approach each other, we exclude coupled-type flutter from the list of possible sources of vibrations.

If the first four sources of high-amplitude plate vibrations are excluded, we will conclude that single mode plate flutter occurs.

4. Theoretical flutter predictions

The plate size was chosen such that coupled-type flutter would not occur. The critical Mach number for coupled-type flutter was computed by applying formula (6) (Movchan, 1957) obtained through piston theory. The static pressure in the wind tunnel changes with change of actual Mach number M. Using this isentropic formula

$$p(M) = p_0\left(1 + (\gamma - 1)\frac{M^2}{2}\right)^{-\gamma/(\gamma-1)}$$

and parameter p_0 typical for the wind tunnel used, we obtain the function $M_{cr}(M)$. Eq. (6) has been derived for a pinned plate, which implies M_{cr} is higher for a clamped plate. Fig. 9 shows the plot $M_{cr}(M)$ for parameters of the wind tunnel used, where we can see that $M_{cr} > M$ for any M, and thus coupled-type flutter is impossible.

On the contrary, single mode flutter should arise at the test conditions. For theoretical analysis the method of Vedeneev (2006) briefly described in Section 2.2 is used. Following that paper, for each eigenmode (m,n) [the first

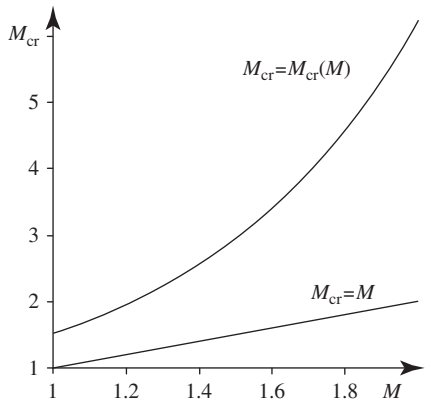

Fig. 9. Plot $M_{cr}(M)$ defined by Eq. (6). Additionally a line $M_{cr} = M$ is shown.

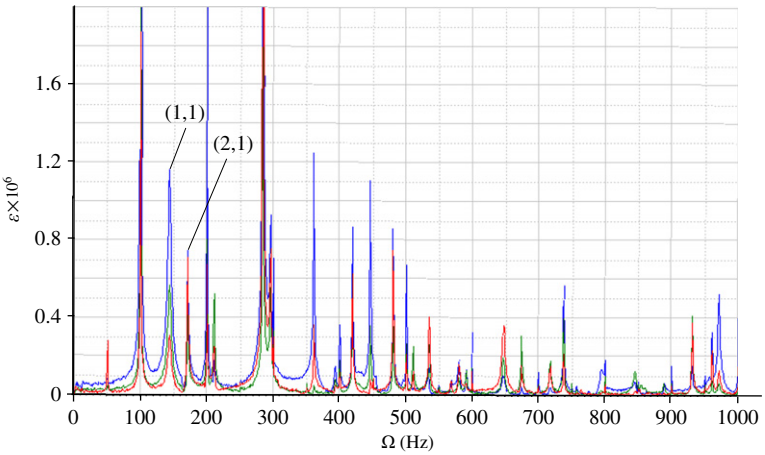

Fig. 10. Spectrum of plate strain gauge data. The plate is excited by slight impact of a mallet. All sharp line peaks with frequencies proportional to 50 and 100 Hz are electrical interferences and should be ignored.

number in brackets is the quantity of half-waves in the mode along the flow (short) direction, the second number is the one along the side (long) direction] there is a region of single mode flutter $M_1(m,n) < M < M_2(m,n)$. We consider only modes fluttering at $M < 1.3$, as the tests were conducted at $M < 1.3$. Calculated values of M_1 and M_2 are presented in Table 1, where $\Omega = \omega/2\pi$ is ordinary frequency.

Thus, during transonic tests in the spectrum of plate oscillations we should see some of seven modes: (1,1), (2,1), (2,2), (3,1), (3,2), (4,1) and (4,2) at corresponding frequencies. More detailed analysis shows that increments of amplification are the biggest for modes (1,1) and (2,1); in other words, these modes are most unstable.

In Table 1 we did not take into account the influence of factors considered in Section 5. Below we will show that the frequency of the mode (1,1) is higher, and this mode should be excited at higher M than presented in the Table 1, while flutter region for the mode (2,1) is the same.

One more test was conducted at $M = 3.0$. Theoretical study shows that despite many natural modes being excited at $M = 3$, the rate of amplification is very low and flutter should be suppressed by the plate material damping. Thus we conclude that no flutter should be observed at $M = 3$.

5. Natural plate oscillations

In order to verify the dynamic properties of the test model produced, initially a free vibration experiment was conducted. A light strike of a mallet was made, while strain gauge data was recorded and analysed. Test spectra are

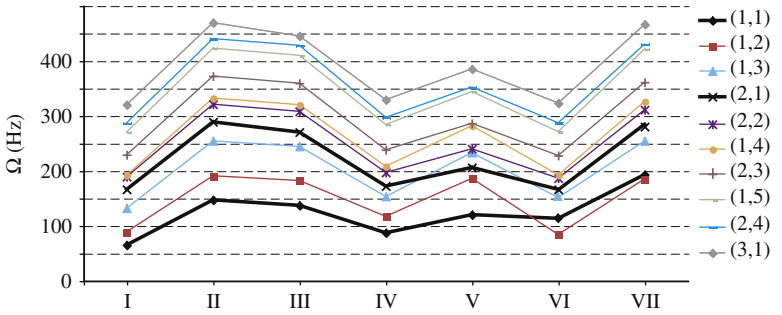

Fig. 11. Influence of non-controllable factors on the plate eigenfrequencies at different load cases. Case I: flat plate; case II: flat plate, temperature (−5 °C); case III: buckled (amplitude 1 mm) plate, temperature (−5 °C); case IV: buckled (amplitude 1 mm) plate; case V: buckled (amplitude 3 mm) plate; case VI: flat plate, with cavity; case VII: flat plate, with cavity, temperature (−5 °C). Modes (1,1) and (2,1) are represented by two bolder curves.

shown in Fig. 10. From a flutter point of view, the most important eigenmodes are (1,1) and (2,1). Test results are 143 Hz for mode (1,1) and 170 Hz for the mode (2,1). The classical formula for a clamped plate eigenfrequencies yields 65 Hz for the mode (1,1) and 167 Hz for the mode (2,1) (see Table 1). We can see that there is an excellent correlation between theory and test data for mode (2,1), while for mode (1,1) there is a paradoxical inconsistency.

In order to understand sources of this inconsistency, the influence on eigenfrequencies of several parameters, not controllable in the test, was studied using ABAQUS finite element software. Several factors influencing natural oscillations, as well as plate vibrations during tests in the wind tunnel, were considered: temperature of the plate, initial out-of-plane deflection, and air pressure in the cavity. Let us consider them in series.

The temperature of the plate can be different from the temperature of other parts of the test assembly. Indeed, when the wind tunnel is just started, cold air flow cools thin plate faster then its thick frame, and temperature strains lead to an increase of eigenfrequencies. With time, the frame also cools, temperature strains disappear, and the eigenfrequencies decrease down to the values of the unstretched plate in vacuum. The plate temperature modelled is −5 °C relative to the frame.

The plate had an out-of-plane static deflection due to residual stresses after welding. Unfortunately, these stresses were not fully eliminated, and the plate was slightly buckled with maximum out-of-plane displacement 2 mm. In the finite element model residual plate deflection was modelled directly: the finite element plate shape was the same as the real plate shape. Two amplitudes of buckling were considered: 1 and 3 mm. Both were modelled, because buckling amplitude could vary or be eliminated during the test because of temperature strains.

The last considered factor, air pressure in the cavity (Fig. 6) is the most interesting one. If the plate oscillates in symmetric eigenmode (for example, at mode (1,1)), then the volume of the cavity, as well as air pressure, changes. Thus the cavity works as an "aerodynamic spring". On the contrary, if the plate oscillates at antisymmetric mode (for example, (2,1)), then the cavity volume does not change, and the cavity does not affect oscillations.

Results of the modelling are shown in Fig. 11. We can see that for free natural oscillations out of the wind tunnel (no temperature effect) the only factor explaining the inconsistency between theory and experiment is the cavity air pressure. Exactly as physical arguments predict, it works as an "aerodynamic spring" for symmetrical oscillation modes, and does not affect antisymmetrical modes. These results also show that residual plate stresses after welding do not affect natural oscillation for the mode (2,1), as the test frequency of this mode is the same as unstressed plate theory predicts.

Fig. 11 also shows the possible behaviour of the plate eigenfrequencies during start-up of the wind tunnel, when the temperature of the plate is lower than the temperature of the frame. We can see that frequencies grow dramatically, even with a slight change of the temperature. This fact is fully confirmed by tests in the wind tunnel: frequencies just after start-up were much higher than frequencies before start-up, and were decreasing with time.

6. Results of the experiment

The test was conducted at twelve regimes of the wind tunnel. The corresponding Mach numbers are $M = 0.857$, 1.147, 1.167, 1.169, 1.285, 1.286, 1.292, 1.293, 1.294, 1.298, and 3.0. These values are intentionally shown with accuracy

0.001. Of course, the pressure gauge and test conditions did not allow to conduct measurements with such a high accuracy. Nevertheless, measuring Mach number in series many times in each regime, we can distinguish with confidence different regimes, despite not being able assert that the Mach number of each regime is measured with accuracy 0.001. Thus, here and below Mach numbers have a relative sense: we can only distinguish the difference between regimes using these values. In other words, despite measured Mach number values being inaccurate, from inequality $M_1' < M_2'$ (where prime denotes an inaccurately measured value) it follows inequality $M_1 < M_2$ for exact test values.

In Figs. 12 and 13 shown are the plate strain amplitudes versus time for two transonic launches of the wind tunnel (in Fig. 13 the first segment represents the unsteady start of the tunnel and must be ignored). Plate strain amplitudes versus

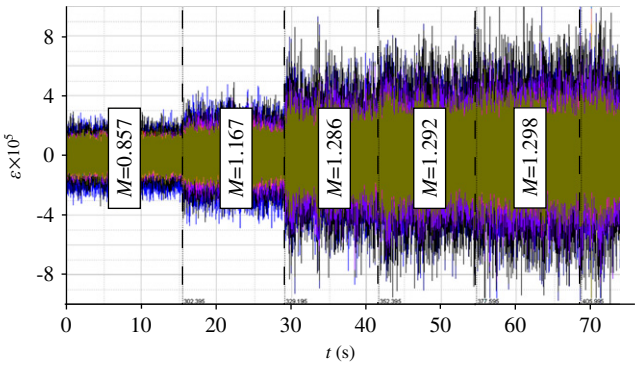

Fig. 12. Amplitude of the plate vibration during launch 1. Wind tunnel vibro gauge failed to register and therefore is not shown.

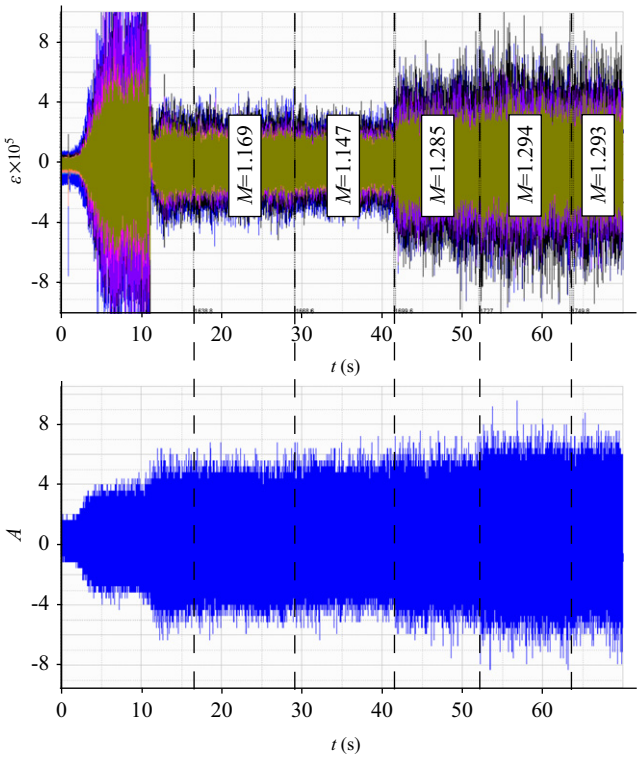

Fig. 13. Amplitude of the plate (top) and the wind tunnel wall (bottom) vibrations during launch 2.

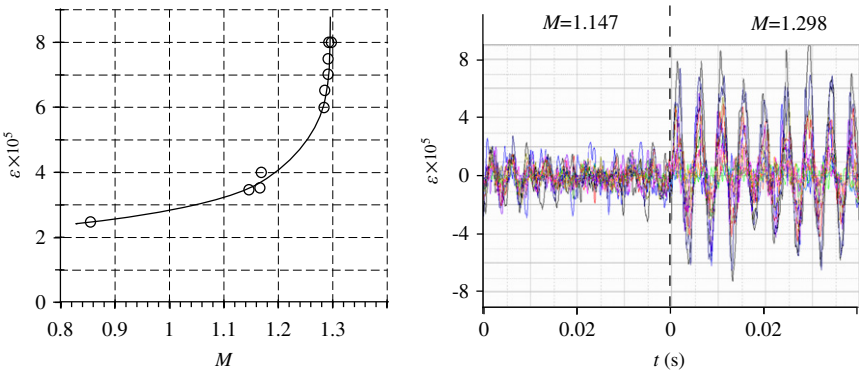

Fig. 14. Left: dynamic strain amplitude versus Mach number. Test data is shown by points, the curve is an interpolation. Right: temporal strain data at $M = 1.147$ (stability) and 1.298 (flutter).

Mach number for these tests are shown in Fig. 14. The most amplitude at $M = 1.298$ in Fig. 14(b) (black curve) corresponds to strain gauge 6 (see Fig. 7).

We can see rapid amplitude growth in region $1.2 < M < 1.3$. Let us now analyze the source of this growth.

In Fig. 15 shown are typical spectra of the plate strain gauges, tunnel vibro gauge, and static pressure gauge. We can see that amplification of the plate oscillations occurs due to amplification of five spectral peaks: 170, 215, 320, 400, and 505 Hz. At the same time, flow pressure and tunnel vibration spectra have no notable spectral peaks in all regimes, and thus plate oscillations are not of the first two types (resonances) specified in Section 3. Note that Fig. 14(b) at $M = 1.298$ shows a frequency of $\Omega = 215$ Hz which corresponds with the (2,1) peak shown in Fig. 15.

Let us now consider the third possible source of amplification of the plate vibrations, noise excitation. If the amplification occurs due to this reason, then noise amplitude (pressure pulsations or tunnel vibrations, depends on which one excites the plate) in different regimes should have the same trend as the plate amplitude. But measurements (using Fig. 13) show that amplitudes of pressure pulsation and tunnel vibrations increase not more than 1.3 times at launch 2, while the plate amplitude increases more than 2 times. Thus, the third source of excitation of the plate vibrations, noise, is also excluded from the list of possible sources.

The fourth source of amplification of the plate vibrations, coupled-mode type flutter, is impossible due to theoretical analysis (Fig. 9). This also can be proved using test data only. Indeed, let us consider the sequence of spectra of plate vibrations with M increasing, shown in Figs. 16 and 15. If coupled-mode type flutter occurs, then, following theory, frequencies of modes (1,1) and (2,1) should approach each other and merge. Analysis of amplitude distribution along the strain gauges shows that in the spectra the peak with frequencies 190 Hz at $M = 1.147$, 180 Hz at $M = 1.167$, 160 Hz at $M = 1.286$, and 170 Hz at $M = 1.298$, corresponds to mode (1,1). Another peak, with frequencies 260 Hz at $M = 1.147$, 230 Hz at $M = 1.167$, 200 Hz at $M = 1.286$, and 215 Hz at $M = 1.298$, corresponds to the mode (2,1). We see that these peaks move along the spectra with change of M due to plate temperature effects, but they do not approach each other. That is why there is no coupled-mode type flutter.

Thus, all items, except single mode flutter, are excluded from the list of possible sources of amplification of plate oscillations listed in Section 3. We therefore conclude that we observe single mode flutter in the region $1.2 < M < 1.3$.

Let us now explain change of the flutter mode frequencies in different regimes. We see that at $M = 0.857$ frequencies of the spectral peaks are higher than the plate eigenfrequencies, as M increases the frequencies go down up to $M = 1.286$, and they go up at higher M. Influence of the cavity cannot be a reason of such a behaviour, as the cavity affects only symmetrical modes, while in the test frequencies of all modes were affected. We suppose that influence of the plate temperature explains such a behaviour. At start-up of the wind tunnel the thin plate cools fast due to cold air, and the frequencies go up during this process. Then the plate frame also cools, temperature strains decrease, and frequencies go down. With M increasing air cools more, and the process repeats.

The launch $M = 3.0$ is shown in Fig. 17 (the first and last segments represent unsteady start-up and shut down of the tunnel and must be ignored). Plate strain amplitude is about 4.5×10^{-5} (compare with Figs. 12 and 13), while the amplitude of the tunnel wall vibration is more than for all transonic regimes. Results of spectral analysis are shown in Fig. 18. The same as previously, spectrum of the tunnel wall vibrations have no notable peaks. We conclude that the tunnel wall vibrations are higher than at transonic regimes, while the plate response is weaker, thus there is no flutter at $M = 3.0$.

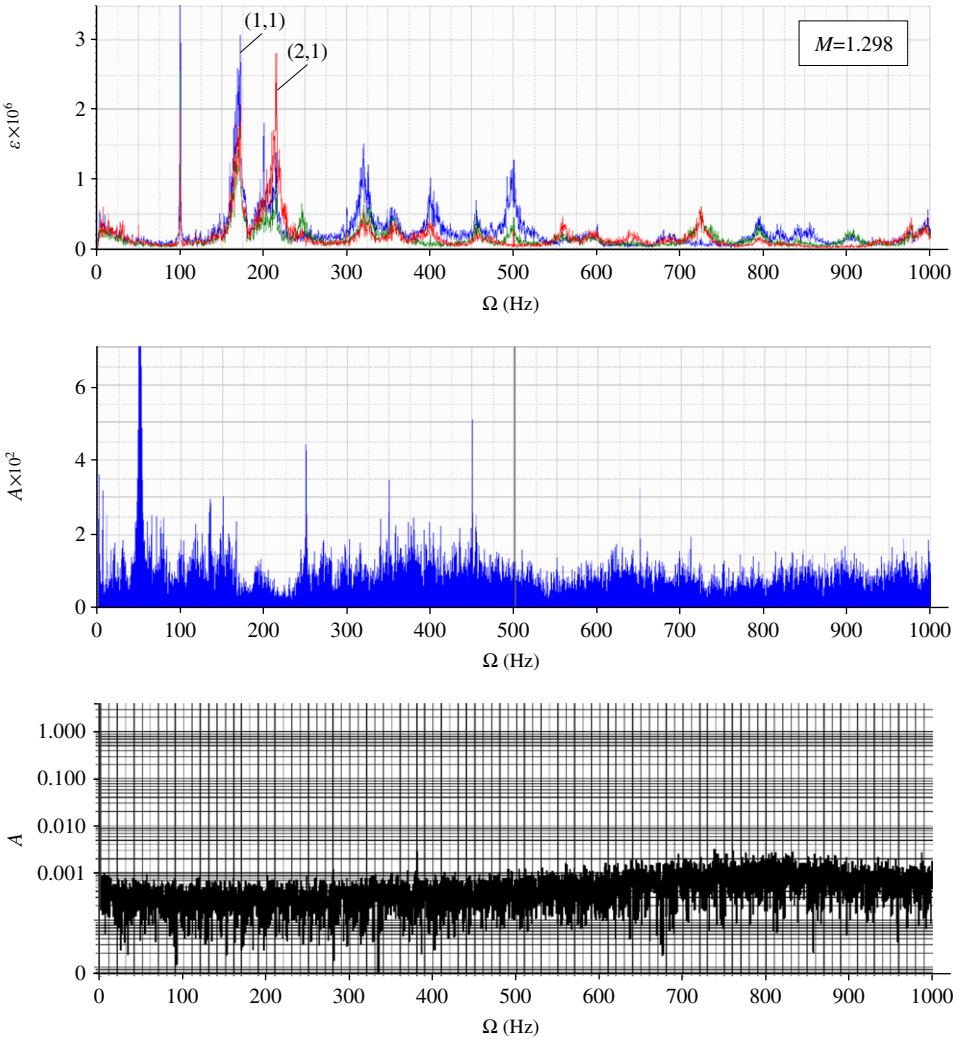

Fig. 15. Spectrum of the plate vibration at regime $M = 1.298$ (top), typical spectrum of the wind tunnel wall vibration (middle), typical spectrum of air pressure pulsation (bottom). All sharp line peaks with frequencies proportional to 50 and 100 Hz are electrical interferences and should be ignored.

7. Comparison with theoretical results

As was theoretically shown in Section 4, for single mode flutter the most unstable modes are (1,1) and (2,1). This is exactly what we see in the test spectra (Figs. 16 and 15): peak lying in region 160–190 Hz corresponds to mode (1,1), peak lying in region 200–260 Hz corresponds to mode (2,1).

The experimental single mode flutter boundary at transonic regimes $M_{cr} \approx 1.2$ is very close to the theoretical value $M_{cr} = \min_{m,n} M_1(m,n) = 1.17$ (Table 1).

Unfortunately, modes of other peaks present in the spectra were not recognized. The reason is residual stresses in the plate left after welding: natural modes were distorted due to the presence of those stresses. Among distorted modes we are not able to distinguish the number of half-waves in modes, because there are no more half-waves. Nevertheless, we have theoretical results in Table 1, and we may assume that other peaks in flutter spectra correspond to some of theoretically unstable modes (2,2), (3,1), (3,2), (4,1), (4,2).

There are two reasons why we are not worried about residual stresses distorting plate eigenmodes. First is the fact that the most unstable modes (1,1) and (2,1) are not really affected by those stresses, and the physical mechanism of single mode flutter excitation (Vedeneev, 2006) described in Section 2.2 works. Another reason is that analysis and

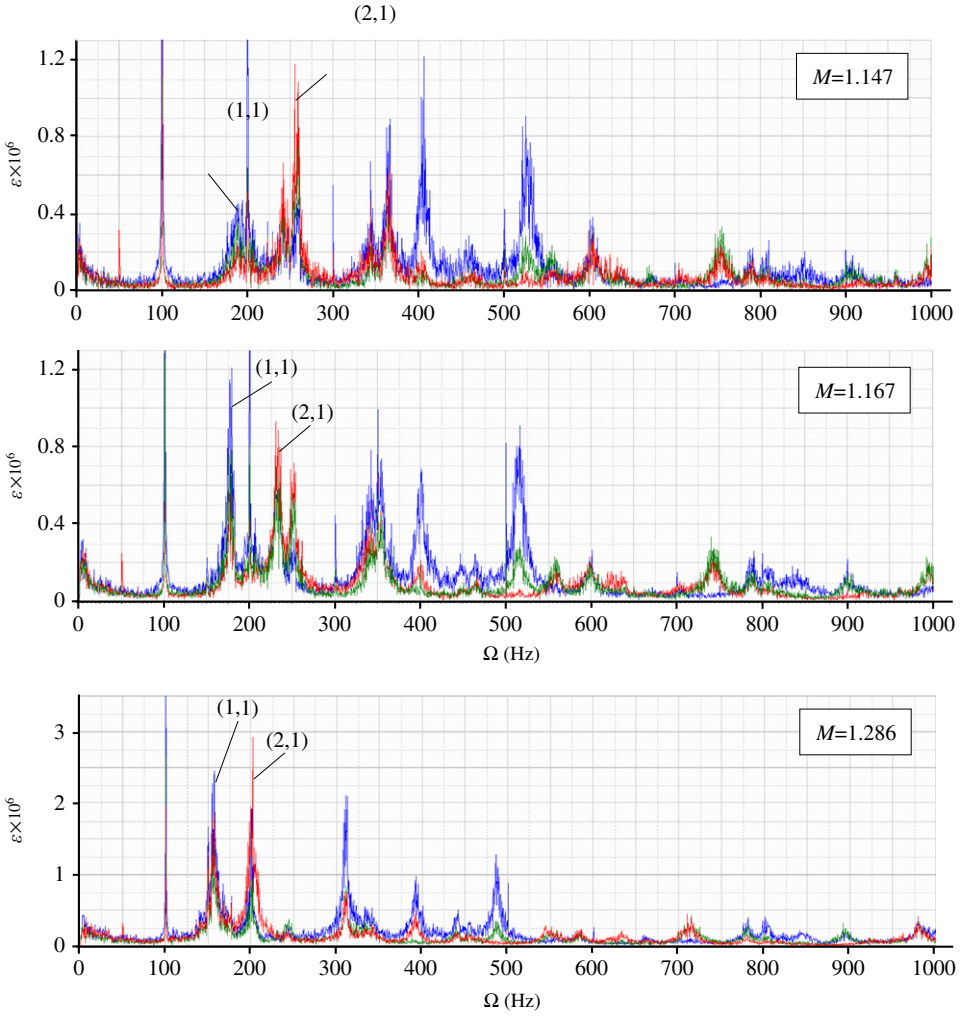

Fig. 16. Spectrum of the plate vibrations at regimes $M = 1.147$, 1.167 and 1.286. All sharp line peaks with frequencies proportional to 50 and 100 Hz are electrical interferences and should be ignored.

conclusions are made through test data only, not utilizing theoretical results. Single mode flutter excitation conclusions are established through investigation of the various types of plate vibrations to be expected as explained in Section 3, and then using only logical arguments based upon the test data to exclude vibration types that are not consistent with the flutter mode experience.

During the launch $M = 3.0$ no flutter was detected. This coincides with theoretical prediction given above.

8. Conclusions

A clamped steel plate is tested in a supersonic wind tunnel. The plate is intentionally chosen so that single mode flutter should occur, while "classical" coupled-mode type flutter is impossible. During the test, plate vibrations amplified in the region $1.2 < M < 1.3$. Analysis of spectra of the plate strain gauges, pressure gauge and wind tunnel vibro gauge showed that the plate experienced single mode flutter.

Test results were in excellent agreement with the theory of Vedeneev (2006): during the tests flutter occurred in modes which are theoretically most unstable. The experimental flutter boundary $M_{cr} \approx 1.2$ is very close to the theoretical value $M_{cr} = 1.17$.

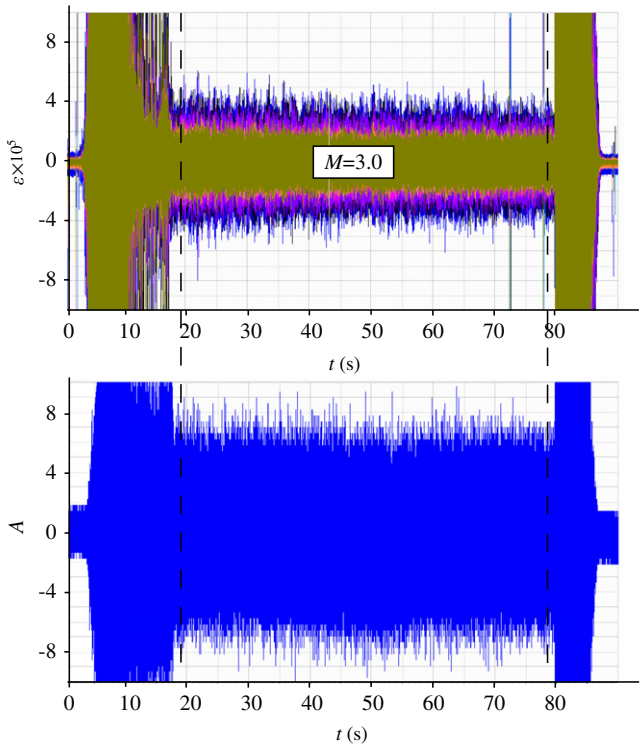

Fig. 17. Amplitude of the plate (top) and the wind tunnel wall (bottom) vibrations during launch 3.

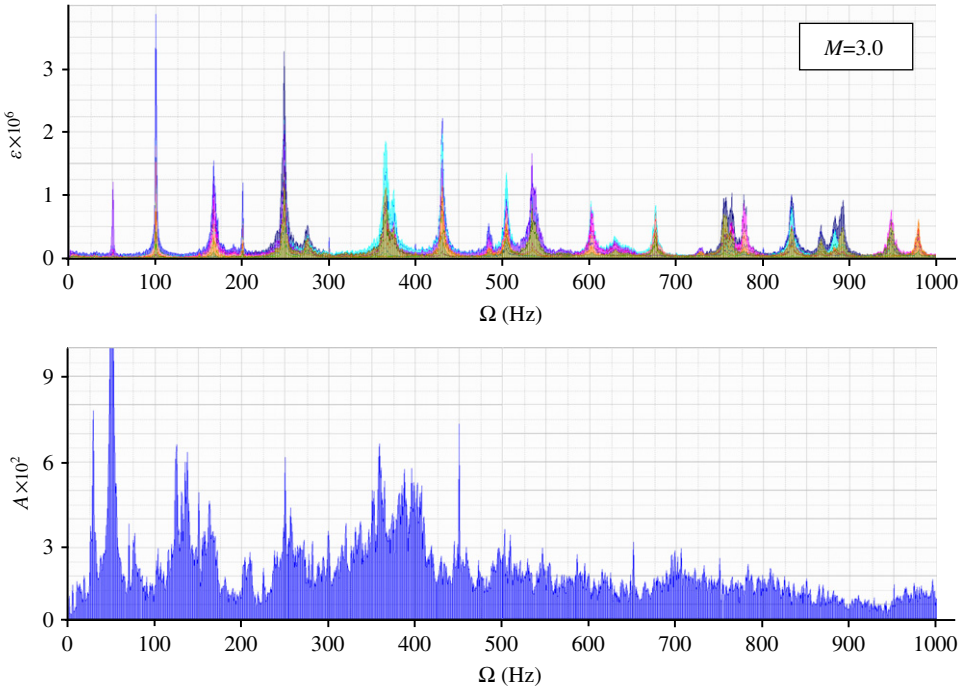

Fig. 18. Spectrum of the plate vibration at regime $M = 3.0$ (top), spectrum of the wind tunnel wall vibration at regime $M = 3.0$ (bottom). All sharp line peaks with frequencies proportional to 50 and 100 Hz are electrical interferences and should be ignored.

In the supersonic regime $M = 3.0$ no flutter was detected. This fact also coincides with theoretical prediction: in theory, there should be single mode flutter, but the rate of the amplitude growth is very slow and flutter should be eliminated by the plate damping.

Acknowledgement

The work is partially supported by Russian Foundation for Basic Research (08-01-00618 and 10-01-00256) and Grants of President of Russian Federation (MK-2313.2009.1 and NSh-4810.2010.1).

References

Bendiksen, O.O., Davis, G.A., 1995. Nonlinear traveling wave flutter of panels in transonic flow. AIAA Paper 95-1486, 17 p.

Bendiksen, O.O., Seber, G., 2008. Fluid-structure interactions with both structural and fluid nonlinearities. Journal of Sound and Vibration 315 (3), 664–684.

Bolotin, V.V., 1963. Nonconservative Problems of the Theory of Elastic Stability. Pergamon Press, Oxford.

Dong Ming-de, 1984. Eigenvalue problem for integro-differential equation of supersonic panel flutter. Applied Mathematics and Mechanics 5 (1), 1029–1040.

Dowell, E.H., 1966. Nonlinear oscillations of fluttering plate. AIAA Journal 4 (7), 1267–1275.

Dowell, E.H., 1967. Nonlinear oscillations of fluttering plate. II. AIAA Journal 5 (10), 1856–1862.

Dowell, E.H., 1971. Generalized aerodynamic forces on a flexible plate undergoing transient motion in a shear flow with an application to panel flutter. AIAA Journal 9 (5), 834–841.

Dowell, E.H., 1974. Aeroelasticity of Plates and Shells. Noordhoff International Publishing, Leyden.

Dowell, E.H., Voss, H.M., 1965. Theoretical and experimental panel flutter studies in the Mach number range 1.0 to 5.0. AIAA Journal 3 (12), 2292–2304.

Dugundji, J., 1966. Theoretical considerations of panel flutter at high supersonic Mach numbers. AIAA Journal 4 (7), 1257–1266.

Dun Mingde, 1958. On the stability of elastic plates in a supersonic stream. Soviet Physics Doklady 3, 479–482.

Gaspers, P.A., Jr., Muhlstein, L., Jr., Petroff, D.N., 1970. Further results on the influence of the turbulent boundary layer on panel flutter. NASA TN D-5798.

Hedgepeth, J.M., 1957. Flutter of rectangular simply supported panels at high supersonic speeds. Journal of the Aeronautical Sciences 24 (8), 563–573 586.

Kulikovskii, A.G., 1966. On the stability of homogeneous states. Journal of Applied Mathematics and Mechanics 30 (1), 180–187.

Kulikovskii, A.G., 2006. The global instability of uniform flows in non-one-dimensional regions. Journal of Applied Mathematics and Mechanics 70 (2), 229–234.

Mei, C., Abdel-Motagaly, K., Chen, R.R., 1999. Review of nonlinear panel flutter at supersonic and hypersonic speeds. Applied Mechanics Reviews 10, 321–332.

Mikishev, G.N., 1959. Experimental research of natural oscillations of a square plate in a supersonic flow. Izvestiya AN SSSR, Mekhanika i mashinostroenie 1, 154–157 (in Russian).

Movchan, A.A., 1957. On stability of a panel moving in a gas. PMM 21 (2), 231–243 (in Russian).

Muhlstein, L., Jr., Gaspers, P.A., Jr., Riddle, D.W., 1968. An experimental study of the influence of the turbulent boundary layer on panel flutter. NASA TN D-4486.

Nelson, H.C., Cunnigham, H.J., 1956. Theoretical investigation of flutter of two-dimensional flat panels with one surface exposed to supersonic potential flow. NACA Report no. 1280.

Vedeneev, V.V., 2005. Flutter of a wide strip plate in a supersonic gas flow. Fluid Dynamics 5, 805–817.

Vedeneev, V.V., 2006. High-frequency flutter of a rectangular plate. Fluid Dynamics 4, 641–648.

Vedeneev, V.V., 2007. Nonlinear high-frequency flutter of a plate. Fluid Dynamics 5, 858–868.

Vedeneev, V.V., 2009. Numerical investigation of supersonic plate flutter using the exact aerodynamic theory. Fluid Dynamics 2, 314–321.

Yang, T.Y., 1975. Flutter of flat finite element panels in supersonic potential flow. AIAA Journal 13 (11), 1502–1507.